

## Stimulation of VTA dopamine inputs to LH upregulates orexin neuronal activity in a D<sub>2</sub>R-dependent manner

Masaya Harada<sup>1</sup>, Laia Serratosa Capdevila<sup>1</sup>, Maria Wilhelm<sup>1</sup>, Denis Burdakov<sup>2,3</sup>, Tommaso Patriarchi<sup>1,2,\*</sup>

<sup>1</sup> Institute of Pharmacology and Toxicology, University of Zürich, Zürich, Switzerland;

<sup>2</sup> Neuroscience Center Zürich, University and ETH Zürich, Zürich, Switzerland;

<sup>3</sup> Department of Health Sciences and Technology, ETH Zürich, Zürich, Switzerland.

\*correspondence to: patriarchi@pharma.uzh.ch

Keywords: orexins, dopamine, Pavlovian, reward, hypothalamus

### Highlights

- Optical VTA DA neuron stimulation is sufficient to elicit a Pavlovian-like dopamine transient in the NAc
- Dopamine in the LH encodes both negative and positive reward prediction errors
- Dopamine in the LH positively modulates orexin neuronal activity locally in a D<sub>2</sub>R dependent way

### Abstract

Dopamine and orexins (hypocretins) play important roles in regulating reward-seeking behaviors. It is known that hypothalamic orexinergic neurons project to dopamine neurons in the ventral tegmental area (VTA), where they can stimulate dopaminergic neuronal activity. Although there are reciprocal connections between dopaminergic and orexinergic systems, whether and how dopamine regulates the activity of orexin neurons is currently not known. Here we implemented an opto-Pavlovian task in which mice learn to associate a sensory cue with optogenetic dopamine neuron stimulation to investigate the relationship between dopamine release and orexin neuron activity in the LH. We found that dopamine release can be evoked in LH upon optogenetic stimulation of VTA dopamine neurons, and is also naturally evoked by cue presentation after opto-Pavlovian learning. Furthermore, orexin neuron activity could also be upregulated by local stimulation of dopaminergic terminals in the LH in a way that is partially dependent on dopamine D<sub>2</sub> receptors (D<sub>2</sub>R). Our results reveal previously unknown orexinergic coding of reward expectation and unveil an orexin-regulatory axis mediated by local dopamine inputs in the LH.

## Introduction

Dopamine in the ventral and dorsal striatum shapes reward-related behaviors<sup>1–5</sup>; its dysregulation has been associated with several psychiatric disorders, including addiction<sup>6–8</sup> and depression<sup>9–11</sup>. It is known that rewarding stimuli evoke dopamine transients both in the ventral<sup>12,13</sup> and dorsal striatum<sup>14</sup>, and that the stimulation of dopaminergic neurons<sup>15,16</sup> or terminals<sup>3</sup> in the striatum is sufficient to trigger operant or Pavlovian conditioning<sup>17</sup> as well as conditioned place preference. Instead, aversive stimuli or omission of expected reward delivery cause a decrease in dopamine in the ventral striatum, resulting in negative reinforcement learning<sup>18,19</sup> via D2 receptors<sup>20,21</sup>.

Although the role of the dopaminergic projections to the striatum or mesolimbic dopamine pathway has been investigated extensively<sup>12,22</sup> – their role in encoding reward prediction errors (RPE) in particular has been a point of focus<sup>12,23</sup> – the role of dopamine in other brain regions is relatively understudied<sup>24–27</sup>. The lateral hypothalamus (LH) plays a pivotal role in reward-seeking behavior<sup>28–32</sup> and feeding<sup>33–36</sup>, and several dopamine receptors are reported to be expressed in the LH<sup>37</sup>. The mechanism through which dopamine modulates neuronal activity in the LH, resulting in the modulation of behaviors, has not been established. To the best of our knowledge, there have been no measurements of dopamine transients in the LH during reward-associated behaviors.

The LH is a heterogeneous structure containing glutamatergic and GABAergic neurons, as well as several neuropeptidergic neurons, such as melanin-concentrating hormone positive and orexin-positive neurons<sup>38,39</sup>. Like dopamine, orexins (also known as hypocretins) are reported to play a pivotal role in reward-seeking behavior<sup>29,40,41</sup>. Orexinergic and dopaminergic systems are known to have reciprocal connections with each other, and some orexinergic neurons project to dopaminergic neurons in the ventral tegmental area (VTA), positively modulating their activity<sup>42,43</sup>. While there has been extensive investigation into how dopamine modulates orexinergic neuronal activity *ex vivo* (*i.e.* acute brain slices)<sup>44–47</sup>, it remains unclear whether and how dopamine transients modulate orexin neuronal activity *in vivo*<sup>47</sup>. Advancements in optical tools, such as optogenetics for manipulating dopamine neurons and genetically encoded dopamine sensors for monitoring dopamine transients, have made it possible to precisely control and observe the dynamics of dopamine in neural systems<sup>13,48–52</sup>. Here, we implemented an ‘opto-Pavlovian task’<sup>17</sup>, in which mice learn to associate a sensory cue with optogenetic dopamine neuron stimulation. Using this task we measured dopamine transients in the nucleus accumbens (NAc), finding that dopamine activity patterns are consistent with previous reports of RPE-encoding dopaminergic neuron activity<sup>22</sup>. Using the same paradigm, we found that optical stimulation of dopaminergic neurons in the VTA evokes an increase of extrasynaptic dopamine in the LH, where the delivery of a cue preceding a reward also triggers dopamine transients in a way that is consistent with RPEs<sup>23</sup>. Furthermore, we investigated the regulation of LH orexinergic neurons by VTA dopaminergic neurons, and observed a dopamine transient in the LH and an increase in orexinergic neuronal activity during both predictive cue and the delivery of laser stimulation, indicating that the concentration of extrasynaptic dopamine in the LH and orexinergic neuronal activity are positively correlated. Finally, by stimulating dopaminergic terminals in the LH combined with pharmacological intervention, we found that dopamine in the LH positively modulates orexinergic neurons via the type 2 dopamine receptor (D2).

Overall, our study sheds light on the meso-hypothalamic dopaminergic pathway, and its impact on orexinergic neurons.

## Results

## RPE-like dopamine transient in the NAc in response to VTA dopamine neuron stimulation

Previous work established an optogenetics-powered Pavlovian conditioning task (hereon called opto-Pavlovian) wherein animals learn to associate the delivery of a cue with optogenetic activation of their midbrain dopamine neurons<sup>17</sup>. This previous study determines that dopaminergic neuron responses to optical stimulation-predictive cues become established over multiple learning sessions. However, in light of recent evidence demonstrating that dopamine release in the mesolimbic system and dopamine neuron activity can be uncoupled we sought out to determine whether dopamine release would also follow the same patterns of dopamine somatic activity during this task<sup>53,54</sup>. To selectively stimulate and monitor dopamine release from ventral tegmental area (VTA) dopaminergic neurons in the nucleus accumbens (NAc), we injected a cre-dependent ChrimsonR AAV in the VTA as well as dLight1.3b<sup>13</sup>, a genetically encoded dopamine sensor AAV, in the NAc of DAT-cre mice. The recording optic fiber was placed directly above the NAc injection site (Figure 1A). Mice then underwent the ‘opto-Pavlovian task’<sup>17</sup>, where one cue (tone+light, 7s) was paired with the optogenetic stimulation of dopamine neurons in the VTA (Figure 1D), while the other cue was not (Figure 1B and Figure 1 - Figure Supplement 1). We observed a gradual increase of dopamine transients in response to the delivery of the laser-associated cue (Figure 1C,E and F). In contrast, the change of response to the non-laser-paired cue was smaller (Figure 1C,E and F), suggesting that mice discriminated between the two cues. After 10 sessions of the opto-Pavlovian task, mice were exposed to omission sessions (Figure 2A), in which one-third of the laser-paired cues failed to trigger laser stimulation and the other two-thirds were followed by laser stimulation of VTA dopamine neurons (Figure 2A, B and C). The omission of the laser stimulation triggered a dip of dLight signal (Figure 2D). We also observed a small dip of dLight signal during non-laser paired cue delivery (Figure 2-figure supplement 1). Overall, the dopamine transient observed during the opto-Pavlovian task was consistent with classical Pavlovian conditioning<sup>17,22</sup>, indicating that mice engage similar learning processes whether the reward consists of an edible entity or of optogenetic stimulation of VTA dopamine neurons.

## Dopamine transients in the LH follow the same rules as in the NAc

Given the involvement of the lateral hypothalamus (LH) in reward-seeking behaviors<sup>28,55</sup>, we next asked whether a similar neuromodulatory coding of predictive cues could take place in the hypothalamus, outside of the mesolimbic dopamine system. To answer this question, we followed the same procedure as for the NAc, except injecting dLight1.3 and positioning the optic fiber for photometry recordings in the LH (Figure 3A). We observed Chrimson positive fibers in the LH originating from the VTA (Figure 3A) and found that the stimulation of VTA dopamine neurons reliably evoked dopamine transients in the LH (Figure 3B). The injected mice expressing dLight1.3b in the LH then underwent the opto-Pavlovian task (Figure 3C-G). On session 1 of the task, we observed dopamine transients neither around laser-paired cue nor around non-laser-paired cue presentation (Figure 3C and D). However, in the LH as in the NAc, there was a gradual increase of dopamine transients around the laser-paired cue delivery (Figure 3 E,F and G), consistent with RPE-like dopamine transients. Omission sessions after 10 sessions of the task (Figure 3H) showed a dip of dopamine signal during omission trials (Figure 3H). These results are indicative of the presence of a certain amount of tonic dopamine in the LH under unstimulated conditions and that negative RPEs can induce a decrease in the concentration of LH dopamine. Interestingly, the dopamine transients in the LH observed in these experiments mirrored the RPE-encoding dopamine responses we observed in the NAc.

## Different kinetics of dopamine in the NAc and LH

After conducting dLight recordings in the NAc and LH during the opto-pavlovian task, we observed distinct kinetics of dopamine in these two brain regions. First we compared the dopamine transient during stimulation trials of omission sessions, where mice already learned the association between the cue and the laser stimulation (Figure 4A). In the NAc, the dLight signal continued to increase until the laser was turned off, while in the LH, the dLight signal plateaued shortly after the initiation of the laser stimulation (Figure 4A). To precisely assess the kinetics of the dLight signals, we calculated their temporal derivatives (Figure 4B). In the NAc, the derivative crossed zero shortly after the termination of the laser stimulation, while in the LH, the zero-crossing point was observed during the laser stimulation (Figure 4B and C), indicating a different timing of direction change in the dLight signal. We applied the same analysis to the omission trials (Figure 4D, E, and F). Following the initiation of the laser-paired cue, two zero-crossing points of the derivative of the dLight signal were identified. The first one corresponded to the maximum of the dLight signal, and the second one corresponded to the minimum of the dLight signal. In the LH, both zero-crossing points were smaller than in the NAc, suggesting that LH dopamine exhibits faster kinetics.

## Orexin neuron dynamics during the opto-Pavlovian task

We next addressed the hypothesis positing that dopamine in the LH can modulate orexinergic neuronal activity. We injected DAT-cre mice with an orexin promoter-driven GCaMP6s<sup>56-59</sup>, which has been reported to target orexin neurons with >96% specificity<sup>59</sup>, in the LH and used fiber photometry to monitor the calcium transients of LH orexinergic neurons while optically controlling dopamine release via ChrimsonR expressed in the VTA (Figure 5A and B). After the mice fully recovered from the surgery, they underwent the opto-Pavlovian task. On session 1, calcium transients in orexin neurons were not modulated by the presentation of laser-paired or non-laser-paired cues (Figure 5C), although laser stimulation triggered the increase of calcium signal (Figure 5 - Figure Supplement 1). As we observed with dLight recordings in the NAc and LH, the orexin-specific GCaMP signal increased across sessions around the presentation of the laser-paired cue (Figure 5D and E), therefore following a similar time course to the evolution of dopamine release in the LH. After mice learned the association, we tested the omission of laser stimulation (Figure 5F). Unlike dopamine signals, we did not observe a dip in orexin activity during omission trials (Figure 5F). Orexin neuron activity is known to be associated with animal locomotion<sup>60,61</sup>. To exclude the possibility that the increase in calcium signaling during laser-paired cue trials is an indirect effect of stimulation-induced locomotion<sup>60,61</sup>, we performed photometry recordings and optogenetic stimulation of VTA dopaminergic terminals in the LH both in freely-moving or in isoflurane-anesthetized conditions (Figure 6A). In both conditions we observed an increased orexinergic neuron activity after the onset of laser stimulation (Figure 6B and C), suggesting that the observed upregulation in orexinergic neuronal activity is independent from animal locomotion. Finally, to identify which dopamine receptor is responsible for this increase in orexinergic calcium, we systemically (I.P.) injected a D1 (SCH 23390) or D2 (raclopride) receptor antagonist, and optically stimulated dopaminergic terminals in the LH (Figure 6E and Figure 6 - Figure Supplement 1). Raclopride largely reduced the observed orexin neuronal activity increases while SCH 23390 did not, indicating that the signal is at least in part mediated by the D2 receptor (Figure 6F). Our experiments suggest that LH orexin neurons participate in the LH response to VTA dopamine, and that D2 receptors play

an important role locally in the LH in regulating orexin neuron activity evoked by dopamine release.

## Discussion

The mesolimbic dopamine system has been proposed to encode reward prediction errors (RPEs)<sup>12,22,23</sup>, which signal a discrepancy between expected and experienced rewards. Recently, it has been demonstrated that the optical stimulation of midbrain dopamine neurons is sufficient to create Pavlovian conditioning<sup>17</sup>. While it is known that cells within the LH express several different dopamine receptor subtypes<sup>37</sup>, and microinjection of D1 and D2 receptor agonists have been shown to decrease food intake in rodents<sup>62</sup>, before our study, dopamine transients in the LH during reward associated tasks had not been reported. Here, we used an opto-Pavlovian task that echoed, with NAc dopamine measurements, already reported findings on the midbrain dopamine neurons' RPE-encoding role<sup>17</sup>. Then, we determined that VTA dopaminergic neurons release dopamine in the LH and found that dopamine transients in the LH in response to the same opto-Pavlovian task were qualitatively similar to those observed in the mesolimbic dopamine system.

Recent findings suggest that dopaminergic transients in the dorsal bed nucleus of the stria terminalis (dBNST) encode RPE<sup>26</sup>, indicating qualitative similarities in dopamine activity within this brain region compared to what we observed in the LH and NAc. Conversely, dopamine responses in other brain regions, such as the medial prefrontal cortex (mPFC)<sup>25,63</sup> and amygdala<sup>50,64</sup>, predominantly react to aversive stimuli. Furthermore, we have found that dopamine in the LH also encodes RPE. However, the specific response of dopamine in the LH to aversive stimuli has not been fully explored, despite existing reports of significant orexinergic activity in response to such stimuli.<sup>65</sup> This gap highlights the need for a detailed examination of how dopamine behaves in the LH when faced with aversive stimuli.

Indeed, during the opto-Pavlovian task, in which we stimulated VTA dopamine neurons and measured dopamine, we observed dopamine transients around a Pavlovian laser-paired cue presentation. We also observed a dip of dLight signal during omission trials, suggesting that a detectable concentration of dopamine is at extrasynaptic space in the LH at basal condition and that at the moment of omission, the concentration of extrasynaptic dopamine decreases. These data indicate that dopamine transients in the LH, as in the NAc, could be encoding reward prediction error.

While smaller than the response to the laser-paired cue, we observed modulation of the dLight signal in the NAc during the presentation of the non-laser paired cue. In Session 1, the cue presentation immediately triggered a dip, whereas in Session 10, it evoked a slight increase in the signal, followed by a dip. Our hypothesis suggests that two components contribute to the dip in the signal. The first is the aversiveness of the cue; the relatively loud sound (90dB) used for the cue could be mildly aversive to the experimental animals. Previous studies have shown that aversive stimuli induce a dip in dopamine levels in the NAc, although this effect varies across subregions<sup>3,63</sup>. The second component is related to reward prediction error. While the non-laser paired cue never elicited the laser stimulation, it shares similarities with the laser-paired cue in terms of a loud tone and the same color of the visual cue (albeit spatially different). We posit that it is possible that the reward-related neuronal circuit was slightly activated by the non-laser paired cue. Indeed, a small increase in the signal was observed on day 10 but not on day 1. If our hypothesis holds true, as this signal is induced by two components, further analysis unfortunately becomes challenging.

While dopaminergic transients in the NAc and LH share qualitative similarities, the kinetics of dopamine differs between these two brain regions. Under optical stimulation, the dLight signal in the NAc exhibited a continuous increase, never reaching a plateau until the laser was turned off. In contrast, in the LH, the dLight signal reached a plateau shortly after the initiation of the laser stimulation. The distinction in dopamine kinetics was also evident during omission trials, where the dopamine kinetics in the LH were faster than those in the NAc. The molecular mechanisms underlying this difference in kinetics and its impact on behavior remain to be elucidated. Due to this kinetic difference, we employed distinct time windows to capture the dip in the dLight signal during omission trials.

Previous work indicates that orexin neurons project to VTA dopamine neurons<sup>40,42,43</sup>, facilitating dopamine release in the NAc and promoting reward-seeking behavior. However, while it has been demonstrated that systemic injection of dopamine receptor agonists activates orexin neurons<sup>41</sup>, their reciprocal connection with dopaminergic neurons had not yet been investigated *in vivo*<sup>47</sup>. Here, we studied the relationship between orexinergic and dopaminergic activity in the LH and found that LH dopamine transients and orexinergic neuronal activities are positively correlated. Seeing as dopamine-related orexinergic activity was reduced by systemic injections of raclopride, we postulate that dopamine in the LH activates orexin neurons via D2R. D2R couples to Gi proteins<sup>66</sup>, so it is unlikely that dopamine directly activates orexin neurons. Our testable hypothesis is that dopamine modulates orexin neuron activation via a disinhibitory mechanism; for example, GABA interneurons could be inhibited by the activation of D2R, consequently disinhibiting orexin neurons<sup>67,68</sup>. It has been established that D1 receptor expressing medium spiny neurons (D1-MSNs) in the NAc densely project to the LH, especially to GABAergic neurons<sup>33,69</sup>, raising a possibility that dopamine in the LH modulates the presynaptic terminals of D1-MSNs. However, administration of D1R antagonist (SCH 23390) did not block the calcium transient in orexin neurons evoked by the dopaminergic terminal stimulation in the LH, implying that the contribution of D1-MSNs to orexin neuronal activity is minimal in our experimental design. While systemic injections of raclopride effectively reduced dopaminergic terminal stimulation-evoked orexinergic activity, the long-lasting calcium signal remained unaltered (Figure. 6E). This discrepancy could arise from an insufficient blockade of dopamine receptors. For D1R blockade, we administered 1 mg/kg of SCH-23390 5 minutes before recordings. This dose is adequate to induce behavioral phenotypes<sup>70</sup> and block D1R-based dopamine sensors<sup>13</sup>, although higher doses have been used in some studies.<sup>50</sup> To block D2R, we injected 1 mg/kg of raclopride, a dose known to induce hypolocomotion<sup>71</sup>, indicating effective modification of the neuronal circuit. However, these data do not guarantee complete receptor blockade, and it is possible that optical stimulation resulted in high extrasynaptic dopamine concentration, leading to partial receptor binding. Alternatively, this component might be mediated by other neurotransmitters, such as glutamate<sup>72-74</sup> or GABA<sup>75</sup>, which are known to be co-released from dopaminergic terminals.

Several *ex vivo* experiments suggest that dopamine, particularly at high concentrations (50  $\mu$ M or higher), reduces the firing rate of orexin neurons, albeit with a potency significantly lower than that of norepinephrine<sup>44,45</sup> through both direct and indirect mechanisms<sup>46,47</sup>. This apparent discrepancy with our results could be attributed to a different time course of dopamine transients. In slice experiments, the concentration of exogenous dopamine or dopamine agonists is determined by the experimenter and often maintained at high levels for minutes. In contrast, in our experimental setup, dopamine evoked by laser stimulation is degraded/reuptaken as soon as the laser is turned off. This variation in the time course of dopamine transients could contribute to the observed differences in responses to dopamine. Another plausible explanation for this discrepancy is the difference in dopamine concentration. Modulations of synaptic transmission to orexinergic neurons by dopamine are

reported to be concentration-dependent<sup>46</sup>. Despite the brightness of the genetically encoded dopamine sensor following a sigmoidal curve in response to changes in dopamine concentration<sup>13</sup>, estimating dopamine concentration *in vivo* based on the sensor's brightness is not technically feasible. Therefore, it is challenging to determine the exact dopamine concentration achieved by laser stimulation, and it is possible that this concentration differs from the one that triggers the reduction in the firing rate of orexin neurons.

Although presentation of laser-paired cue and laser stimulation of VTA dopamine neurons evoked dopamine transient in the LH and an increase of calcium signals of orexin neurons, we did not observe a dip of calcium signal of orexin neurons during omission trials. This lack of a dip could be due to 1) slow sensor kinetics<sup>76</sup> – since the pre-omission cue triggers LH dopamine release, and increases the calcium transient in orexin neurons, if the kinetics of GCaMP6s expressed in orexin neurons were too slow, we would not be able to observe an omission-related orexin activity dip – 2) dopamine signaling properties. Dopamine receptors couple to G proteins<sup>77</sup>, which act relatively slowly, potentially preventing us from seeing an omission-related signaling dip. Both theories are compatible with our observation that orexinergic activity increases over time during the presentation of our laser-paired cue, as our observed increases are not sporadic but developed over time. Recent studies indicate that orexin neurons respond to cues associated with reward delivery. However, unlike dopaminergic responses, which linearly correlate with the probability of reward delivery, the orexin response plateaus at around 50% probability of reward delivery<sup>56</sup>. This observation indicates that orexin neurons encode multiplexed cognitive information rather than merely signaling reward prediction error. Our data indicate a direct conveyance of dopaminergic information, specifically reward prediction error, to orexinergic neurons. However, the mechanism by which orexinergic neurons process and convey this information to downstream pathways remains an open question.

The silencing of orexinergic neurons induces conditioned place preference<sup>78</sup>, suggesting that the silencing of orexin neurons is positively reinforcing. Considering that the stimulation of VTA dopamine neurons<sup>15,16</sup> and dopaminergic terminals in the LH<sup>79</sup> is generally considered to be positively reinforcing, the activation of orexin neurons by dopaminergic activity might be competing with dopamine's own positive reinforcing effect. At the moment of omission, we observed a dopamine dip both in the NAc and LH, while orexin neurons were still activated. These data suggest that there is a dissociation between dopamine concentration and orexin neuronal activity at the moment of omission. This raises the intriguing possibility that this dissociation - the activation of orexin neurons during a quiet state of dopamine neurons – could be highly aversive to the mice, therefore could be playing a role in negative reinforcement<sup>20,22,39</sup>.

It has been demonstrated that the orexin system plays a critical role in motivated learning<sup>80</sup>. Blocking orexin receptors impairs pavlovian conditioning<sup>81</sup>, operant behavior<sup>82</sup>, and synaptic plasticity induced by cocaine administration<sup>40</sup>. Additionally, dopamine in the LH is essential for model-based learning, and the stimulation of dopaminergic terminals in the LH is sufficient to trigger reinforcement learning<sup>79</sup>. These collective findings strongly suggest that the activation of orexin neurons, evoked by dopamine transients, is crucial for reinforcement learning. Our data indicate that dopamine in both the NAc and LH encodes reward prediction error (RPE). One open question is the existence of such a redundant mechanism. We hypothesize that dopamine in the LH boosts dopamine release via a positive feedback loop between the orexin and dopamine systems. It has already been established that some orexin neurons project to dopaminergic neurons in the VTA, positively modulating firing<sup>42</sup>. On the other hand, our data indicate that dopamine in the LH stimulates orexinergic neurons. These collective findings suggest that when either the orexin or dopamine system

is activated, the other system is also activated consequently, followed by further activation of those systems. Although the current findings align with this idea, the hypothesis should be carefully challenged and scrutinized.

In summary, by implementing an opto-Pavlovian task combined with fiber photometry recordings, we found evidence that the meso-hypothalamic dopamine system exhibits features qualitatively similar to those observed in the mesolimbic dopamine system – where dopamine is thought to encode RPEs. Furthermore, our findings show that dopamine in the LH positively modulates the neuronal activities of orexin neurons via D2 receptors. These findings give us new insights into the reciprocal connections between the orexin and dopamine systems and shed light on the previously overlooked direction of dopamine to orexin signaling, which might be key for understanding negative reinforcement and its dysregulation.

## Methods

### Animals

All animal procedures were performed in accordance to the Animal Welfare Ordinance (TSchV 455.1) of the Swiss Federal Food Safety and Veterinary Office and were approved by the Zurich Cantonal Veterinary Office. Adult DAT-IRES-cre mice (B6.SJL-Slc6a3tm1.1(cre)Bkmn/J; Jackson Labs), referred to as Dat-cre in the manuscript, of both sexes were used in this study. Mice were kept in a temperature- and humidity-controlled environment with ad libitum access to chow and water on 12-h/12-h light/dark cycle.

### Animal surgeries and viral injections

Surgeries were conducted on adult anesthetized mice (males and females, age > 6 weeks). AAV5-hSyn-FLEX-ChrimsonR-tdTomato (UNC Vector Core, 7.8 x 10E12 vg/ml) was injected in the VTA (-3.3 mm AP, 0.9 mm ML, -4.28 mm DV, with 10 degrees angle, volume: 600 nL). Above the injection site, a single optic fiber cannula (diameter: 200  $\mu$ m) was chronically implanted (-3.3 mm AP, 0.9 mm ML, -4.18 mm DV). In the NAc (1.5 mm AP, 0.7 mm ML, -4.5 mm DV), AAV9-hSyn1-dLight1.3b-WPRE-bGHP (Viral Vector Facility, 7.9 x 10E12 vg/ml) was injected and an optic fiber (diameter: 400  $\mu$ m) was implanted (1.5 mm AP, 0.7 mm ML, -4.4 mm DV) for photometry recordings. In some mice, dLight virus or AAV1.pORX.GCaMP6s.hGH<sup>56</sup> was injected in the LH (-1.4 mm AP, 1.1 mm ML, -5.0 mm DV), followed by an optic fiber implantation (-1.4 mm AP, 1.1 mm ML, -4.8 mm DV).

### Opto-Pavlovian task

Dat-cre mice infected with AAV5-hSyn-FLEX-ChrimsonR-tdTomato in the VTA were placed in an operant chamber inside a sound-attenuating box with low illumination (30 Lux). Chamber functions synchronized with laser light deliveries were controlled by custom-written Matlab scripts via a National Instrument board (NI USB 6001). The optic fiber implanted above the VTA was connected to a red laser (638 nm, Doric Lenses; CLDM\_638/120) via an FC/PC fiber cable (M72L02; Thorlabs) and a simple rotary joint (RJ1; Thorlabs). Power at the exit of the patch cord was set to  $15 \pm 1$  mW. Two visual cues were in the operant chamber and a speaker was placed inside the sound-attenuating box. The laser-predictive cue was composed of the illumination of one visual stimulus (7 seconds continuous) and a tone (5kHz, 7 seconds continuous, 90dB), while the non-laser-paired cue was composed of a second visual stimulus (7 seconds continuous) and a different tone (12kHz, 7 seconds continuous, 90dB). Each cue was presented for 7 seconds. Two seconds after the onset of the laser-predictive cue, the red laser was applied for 5 seconds (20Hz, 10ms pulse duration). The presentation of the non-laser cue was followed by no stimuli. In random interval 60 seconds (45-75 seconds), one cue was presented in a pseudorandom sequence (avoiding the presentation of the same trials more than three times in a row). Mice were

exposed to 30 laser cues and 30 Non-laser-paired cues in each session. Mice were trained 5 days per week. After 10 sessions of opto-Pavlovian training, mice underwent 2 sessions of omission. In the omission sessions, two thirds of laser-paired cue presentation was followed by the delivery of the laser stimulation (laser trial), and one third of laser-paired cue presentation didn't lead to laser stimulation (omission trial). The laser-paired cue was kept the same for laser and non-laser trials. Each omission session was composed of 20 laser trials, 10 omission trials, and 30 non-laser trials.

### Photometry recordings

Fiber photometry recordings were performed in all the sessions. Dat-cre mice injected with AAV9-hSyn1-dLight1.3b-WPRE-bGHP in the NAc or LH, or AAV1.pORX.GCaMP6s.hGH in the LH were used. All the mice were infected with AAV5-hSyn-FLEX-ChrimsonR-tdTomato in the VTA. iFCM6\_IE(400-410)\_E1(460-490)\_F1(500-540)\_E2(555-570)\_F2(580-680)\_S photometry system (Doric Lenses) was controlled by the Doric Neuroscience Studio software in all the photometry experiments except for Figure 6's anesthesia experiment. In Figure 6's experiment, a 2-color + optogenetic stimulation rig (Tucker-Davis Technologies, TDT) was used. Mice were exposed to 5% isoflurane for anaesthesia induction, and were kept anesthetized at 2 % isoflurane through the rest of the experiment. The recordings started 10min after the induction of anesthesia. A low-autofluorescence patch cord (400  $\mu$ m, 0.57 N.A., Doric Lenses) was connected to the optic fiber implanted above the NAc or LH. The NAc or LH was illuminated with blue (465 nm, Doric) and violet (405 nm, Doric) filtered excitation LED lights, which were sinusoidally modulated at 208 Hz and 572 Hz (405nm and 465nm, respectively) via lock-in amplification, then demodulated on-line and low-passed filtered at 12 Hz in the Doric system. In the TDT system, signals were sinusoidally modulated, using the TDT Synapse® software and a RX8 Multi I/O Processor at 210 Hz and 330 Hz (405nm and 465nm, respectively) via a lock-in amplification detector, then demodulated on-line and low-passed filtered at 6 Hz. Analysis was performed offline in MATLAB. To calculate  $\Delta F/F_0$ , a linear fit was applied to the 405 nm control signal to align it to the 470 nm signal. This fitted 405 nm signal was used as  $F_0$  in standard  $\Delta F/F_0$  normalization  $\{F(t) - F_0(t)\}/F_0(t)$ . For Figure 5's antagonist experiments, SCH-23390 (1mg/kg in saline) or raclopride (1mg/kg in saline) was injected (I.P.) 5 minutes before recordings.

### Immunohistochemistry

Perfused brains were fixed with 4% Paraformaldehyde (Sigma-Aldrich) overnight (room temperature) and stored in PBS at 4°C for a maximum of one month. Brains were sliced with a Vibratome (Leica VT1200S; feed=60 $\mu$ m, freq=0.5, ampl=1.5), and brain slices near the fiber tracts were subsequently selected for staining. These slices were permeabilized with 0.3% Triton X-100 for 10 min (room temperature). Next, they were incubated with blocking buffer for 1 h (5% bovine serum albumin, BSA; 0.3% Triton x-100) before staining with the respective primary antibodies (NAc and LH with  $\alpha$ GFP chicken 1:1000, Aves Labs ref GFP-1010;  $\alpha$ mCherry rabbit, 1:1000, abcam ab167453; and  $\alpha$ Orexin goat, 1:500, Santa Cruz Biotech, C-19; VTA with  $\alpha$ mCherry rabbit, 1:1000, abcam, ab167453; and  $\alpha$ TH chicken, 1:500, TYH0020) overnight. After three washes with 0.15% Triton, samples were incubated with the respective secondary antibodies and DAPI (for GFP donkey-achicken, 1:1000, AlexaFluor 488, 703-545-155; for mCherry donkey-arabbit 1:67, Cy3, Jackson, 711-165-152; for orexin donkey-agoat, 1:500, Cy5; for TH donkey-achicken, 1:67, AlexaFluor647, 703-605-155; for DAPI 1:2000, ThermoFisher, 62248) for 1h. Finally, samples were washed three times with PBS and mounted on microscope slides with a mounting medium (VectaShield® HardSet™ with DAPI, H-1500-10). Image acquisition was performed with a ZEISS LSM 800 with Airyscan confocal microscope equipped with a Colibri 7 light source (Zeiss Apochromat).

### Statistical Analysis

Statistical analysis was performed in Graphpad Prism9. For all tests, the threshold of statistical significance was placed at 0.05. For experiments involving one subject, one

sample t-test was used. For experiments involving two independent subjects or the same subjects at two different time points, two tailed Student's unpaired or paired t-test was used, respectively. For experiments involving more than two groups, one-way or two-way ANOVA was performed and followed by Tukey's multiple comparison test. All data are shown as mean  $\pm$  SEM.

### **ACKNOWLEDGEMENTS**

We acknowledge funding from the Swiss National Science Foundation (grant agreement: 310030\_196455) (TP), the European Union's Horizon 2020 research and innovation program (grant agreement no. 891959 to TP), and the University of Zürich. We would like to thank Jean-Charles Paterna and the Viral Vector Facility of the Neuroscience Center Zürich (ZNZ) for the kind help with virus production.

### **COMPETING FINANCIAL INTERESTS**

The authors have nothing to disclose.

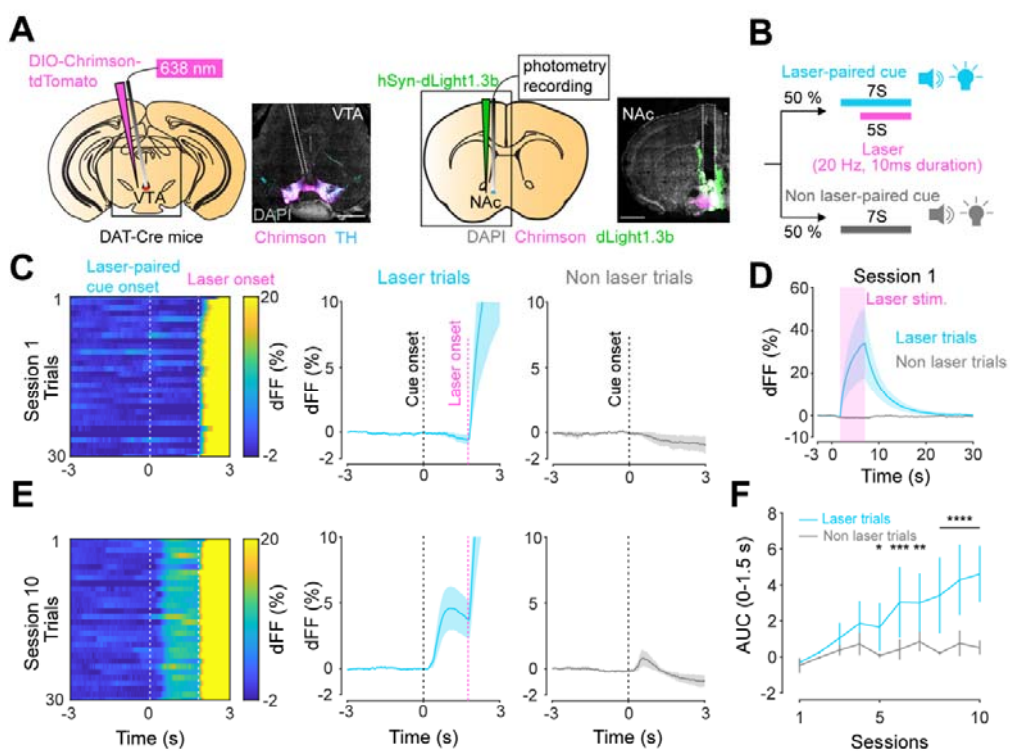


**Figure 1. A.** Preparation for opto-Pavlovian task combined with dLight recordings in the NAc. Scale bar; 1mm. White dashed lines indicate fiber tracts. **B.** Schematic for opto-Pavlovian task. One cue was associated with the laser delivery while the other cue was not. **C.** dLight recordings in the NAc of a representative mouse around the laser-paired cue presentation at session (left) and grouped data (middle). dLight recordings of non laser-paired trials are also shown (right) at session 1. **D.** dLight signals at session 1 during laser stimulation. The signals during non-laser trials are shown also. **E.** The signals of a representative mice around laser-paired cue (left), grouped data (middle) and signals around non-laser paired cue presentation (right) at session 10. **F.** Area under the curve (AUC) of dLight signal in the NAc around the cue presentations (0-1.5 seconds) across sessions. Laser-paired cue triggered bigger transient than non-laser paired cue. 2-way repeated measures ANOVA. Session,  $F_{9,27} = 3.339$ ,  $P=0.0072$ . Cue,  $F_{1,3} = 3.997$ ,  $P=0.139$ . Interaction,  $F_{9,27} = 5.287$ ,  $P=0.0003$ . Tukey's multiple comparison, \* $p<0.05$ , \*\* $p<0.01$ , \*\*\* $p<0.001$  and \*\*\* $p<0.0001$ .  $n=4$  mice.

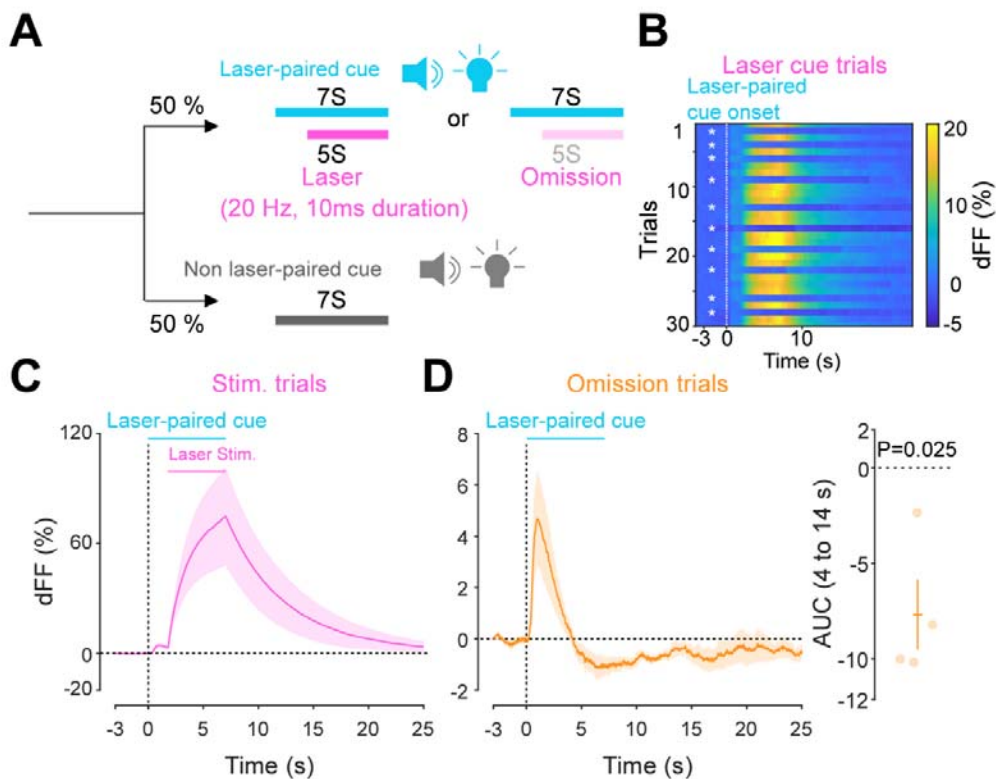


**Figure 2. A.** Schematic for the omission sessions. Two thirds of laser associated cue was followed by the laser stimulation while the other one third of the laser associated cue failed to trigger the laser stimulation. **B.** dLight recordings of a representative mouse during omission sessions. dLight signal around the laser-paired cue presentation is shown here. White asterisks indicate omission trials, while in the other trials, the laser stimulation was delivered. **D.** dLight recordings in the NAc during stimulation trials and during omission trials(**C**). A dip of dLight signals was observed. One sample t test;  $t=4.176$ ,  $df=3$ ,  $P=0.0250$ .  $n=4$  mice.

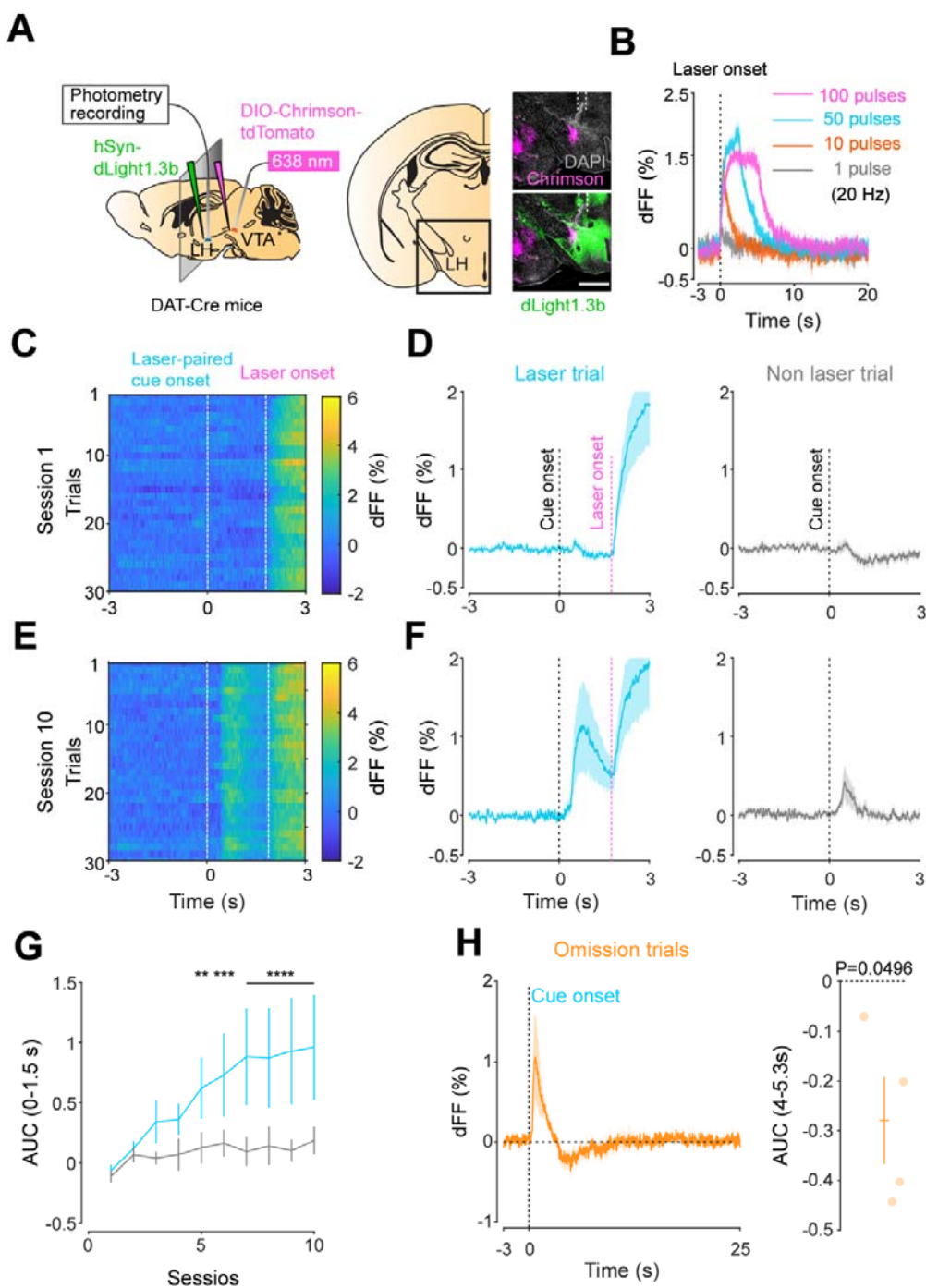


**Figure 3. A.** Schematic for the dLight recording in the LH while stimulating dopamine neurons in the VTA (left). Coronal image of the LH of a mouse infected with AAV-hSyn-DIO-Chrismom-tdTomato in the VTA and AAV-hSyn-dLight1.3b in the LH (right). White dashed lines indicate fiber tracts. Scale bar; 1mm. **B.** dLight signal in the LH during dopaminergic stimulation in the VTA at several number of pulses (20Hz, 10ms duration for each pulse). **C.** dLight recordings during the laser-paired cue presentation of a representative mouse at session 1. **D.** dLight recordings around the laser-paired cue presentation (left) and non-laser-paired cue presentation

(right) at session 1. **E.** dLight recordings during the laser-paired cue presentation of a representative mouse at session 10. **F.** dLight recordings around the laser-paired cue presentation (left) and non-laser-paired cue presentation (right) at session 10. **G.** Area under the curve (AUC) of dLight signal in the LH around the cue presentations (0-1.5 seconds) across sessions. Laser-paired cue triggered bigger transient than non-laser paired cue. 2-way repeated measures ANOVA. Session,  $F_{9, 27} = 3.814$ ,  $P=0.0033$ . Cue,  $F_{1, 3} = 5.818$ ,  $P=0.0948$ . Interaction,  $F_{9, 27} = 3.923$ ,  $P=0.0027$ . Tukey's multiple comparison, \* $p<0.05$ , \*\* $p<0.01$ , \*\*\* $p<0.001$  and \*\*\* $p<0.0001$ . **H.** dLight recordings in the LH during omission trials. A dip of dLight signals was observed. One sample t test;  $t=3.193$ ,  $df=3$ .  $P= 0.0496$ .  $n=4$  mice.

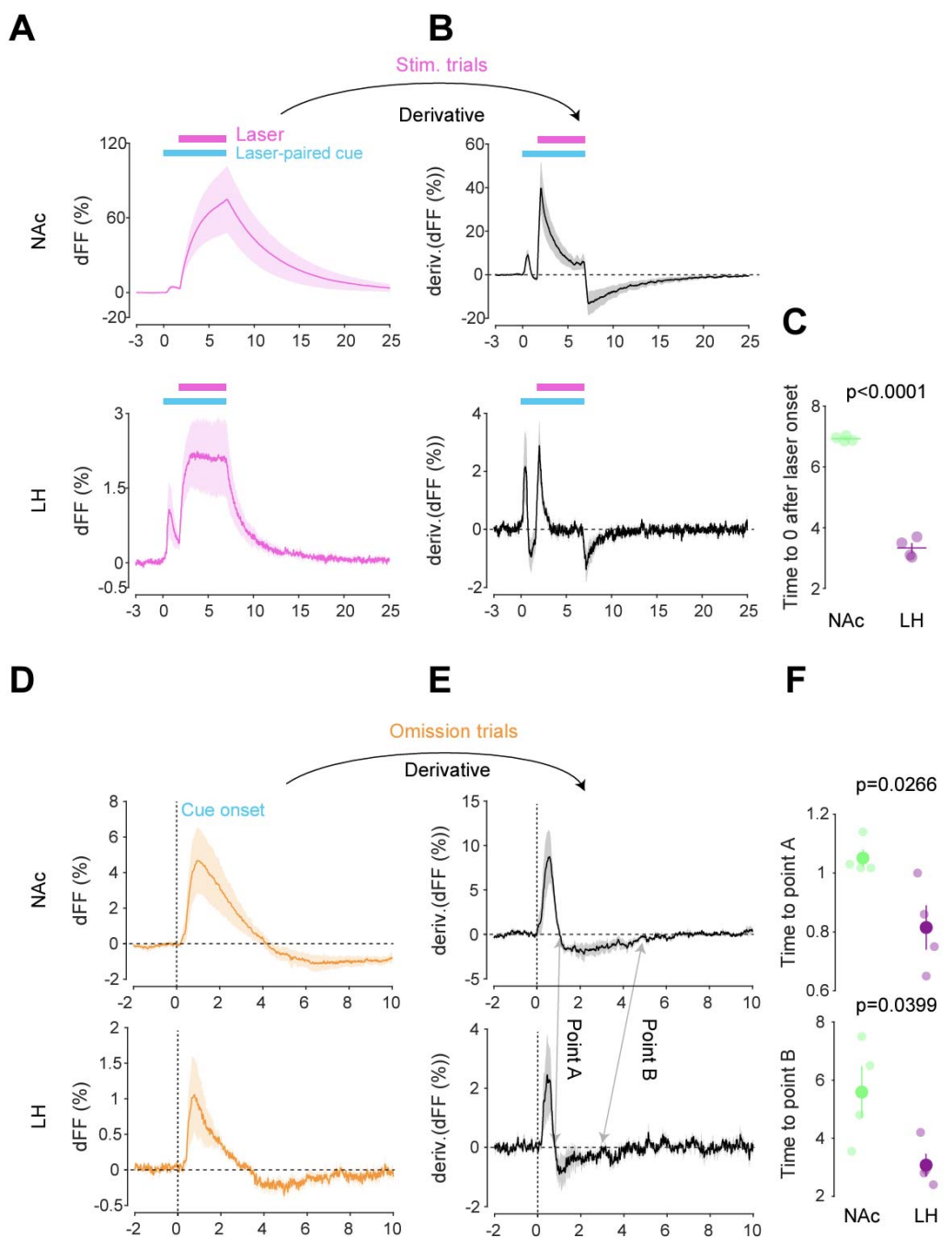


**Figure 4. A.** dLight recordings in the NAc (top) and LH (bottom) during optical stimulation of VTA dopamine neurons. **B.** Derivative of panel A. **C.** quantification of zero-crossing point in panel B after the initiation of laser stimulation. Unpaired t-test;  $t=21.69$ ,  $df=6$ .  $p<0.0001$ . **D.** dLight recordings in the NAc (top) and LH (bottom) during omission trials. **E.** Derivative of panel D. **F.** Quantification of first (top, point A) and second (bottom, point B) zero-crossing points after the initiation of the cue in panel E. Top, unpaired t-test.  $T=2.920$ ,  $df=6$ .  $p=0.0266$ . bottom, unpaired t-test.  $T=2.614$ ,  $df=6$ .  $p=0.0399$ . Note that panels A and D are shown in figure 2 and 3 also. They are displayed for comparison purposes.

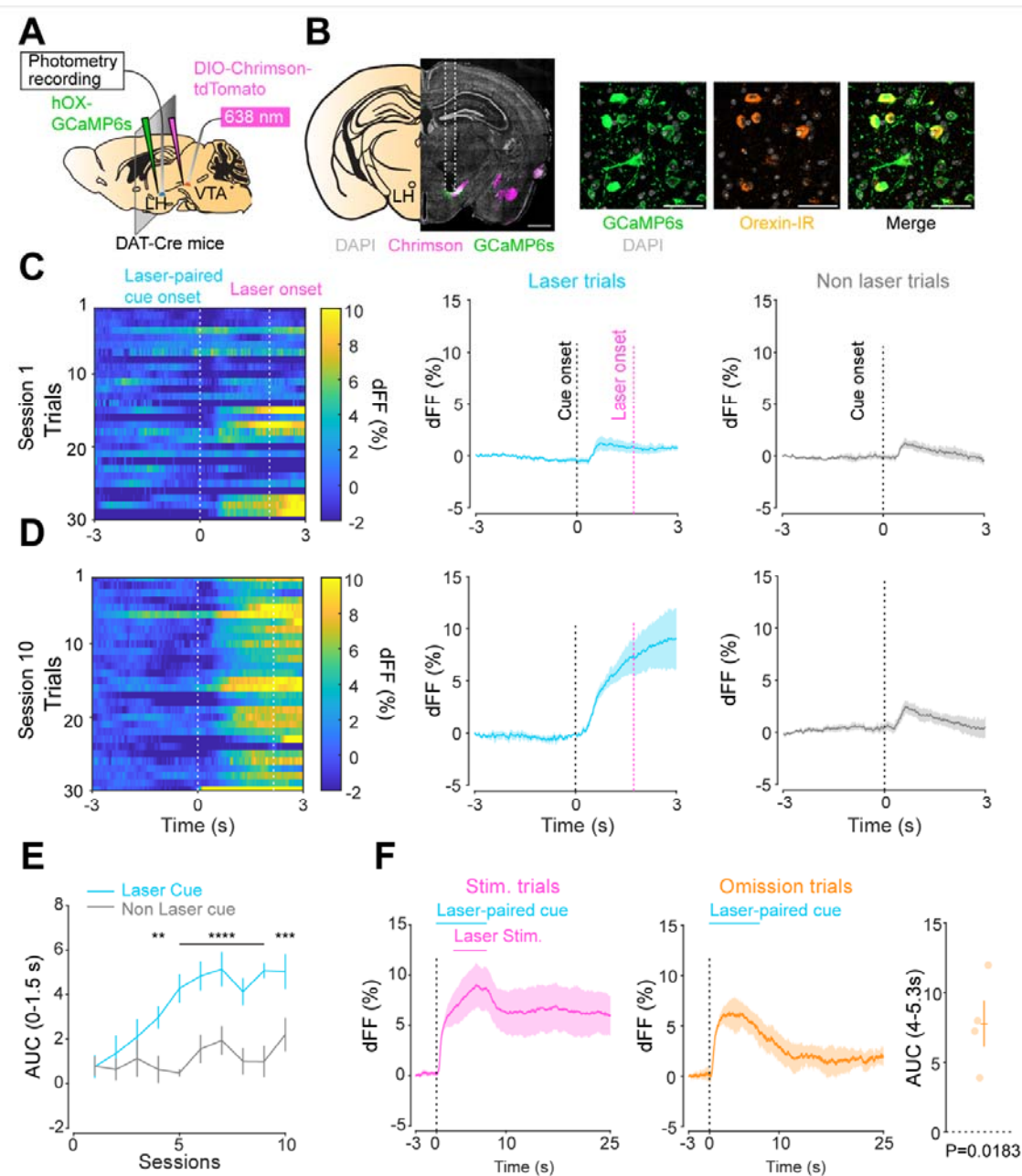


**Figure 5. A.** Schematic of the preparation for opto-Pavlovian task combined with orexin promoter GCaMP recordings in the LH. **B.** Coronal image of a mouse brain slice infected with AAV-hSyn-DIO-ChrismsonR-tdTomato in the VTA and AAV1-hOX-GcaMP6S in the LH (left. Scale Bar; 1mm). White dashed lines indicate fiber tracts. Zoom of infected LH with AAV1-hOX-GcaMP6s and co-localization orexin IR and GcaMP6s (right. Scale Bars; 50  $\mu$ m). **C.** Orexin promoter GcaMP recordings in the LH of a representative mouse around the laser-paired cue presentation at session 1 (left), grouped data (middle) and recordings during non laser-paired trial (right). **D.** Orexin promoter GcaMP recordings in the LH of a representative mouse around the laser-paired cue presentation at session 10 (left), grouped data (middle) and recordings during non laser trial (right). **E.** Area under the curve (AUC) of hOX-

GCaMP signal in the LH around the cue presentations (0-1.5 seconds) across sessions. Laser-paired cue triggered bigger transient than non-laser paired cue. 2-way repeated measures ANOVA. Session,  $F_{9, 27} = 4.438$ ,  $P=0.0012$ . Cue,  $F_{1, 3} = 25.41$ ,  $P=0.0151$ . Interaction,  $F_{9, 27} = 4.125$ ,  $P=0.0020$ . Tukey's multiple comparison, \* $p<0.05$ , \*\* $p<0.01$ , \*\*\* $p<0.001$  and \*\*\* $p<0.0001$ . **F.** Orexin promoter GCaMP recordings during stimulation trials (left) and omission trials (middle and right). AUC around the omission was higher than baseline. One sample t test;  $t=4.693$ ,  $df=3$ .  $P=0.0183$ .  $n=4$  mice.

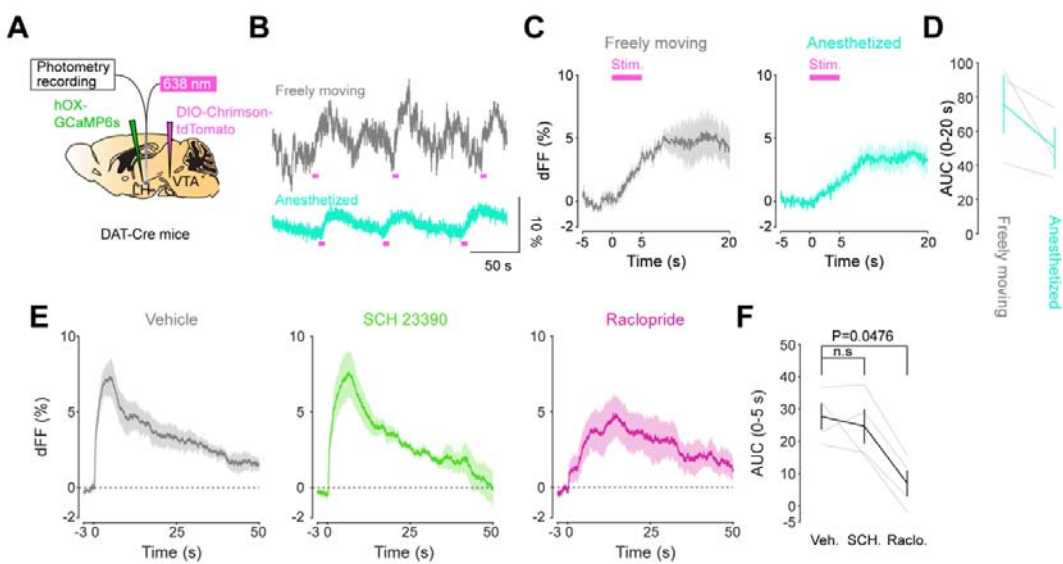


**Figure 6. A.** Schematic for the orexin promoter GCaMP recording in the LH while stimulating dopamine terminals in the LH. **B.** Orexin promoter GCaMP signals of a representative mouse. Recordings were performed while mice were freely moving (top) and anesthetized with isoflurane (bottom). Red bars indicate the stimulation. (20Hz, 100 pulses, 10 ms duration). **C.** Orexin promoter GCaMP signals around the stimulation of dopamine terminals in the LH while animals were freely moving (left) and anesthetized (right). **D.** AUC at 0 to 20 seconds was not significantly different between freely moving and anesthetized conditions. Paired t test,  $t=1.923$   $df=2$ .  $P=0.1944$ .  $n=3$  mice. **E.** In freely moving condition, recordings were performed after mice received the intraperitoneal injection of vehicle (left), SCH 23390 (1mg/kg, middle), and raclopride (1mg/kg, right). **F.** Area under the curve (AUC) at 0-5 seconds. Black line indicates the mean for each condition and grey lines show individual mice. The administration of raclopride decreased the AUC significantly while SCH 23390 did not change the AUC. One-way analysis of variance;  $F(3, 6) = 5.305$ ,  $P=0.04$ . Tukey's multiple comparison test. vehicle vs. SCH 23390;  $P=0.8145$ . vehicle vs. raclopride;  $P=0.0476$ .  $n=4$  mice.

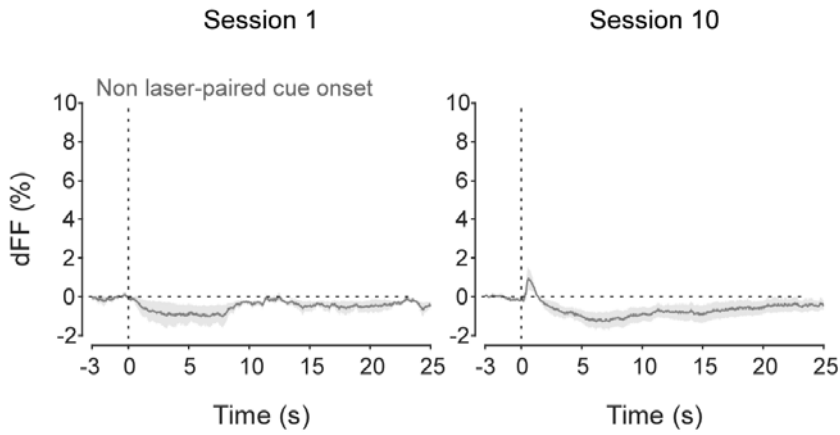


**Figure 1 - Figure Supplement 1.** dLight recordings in the NAc during non-laser-paired cue delivery at session 1 (left) and 10 (right).

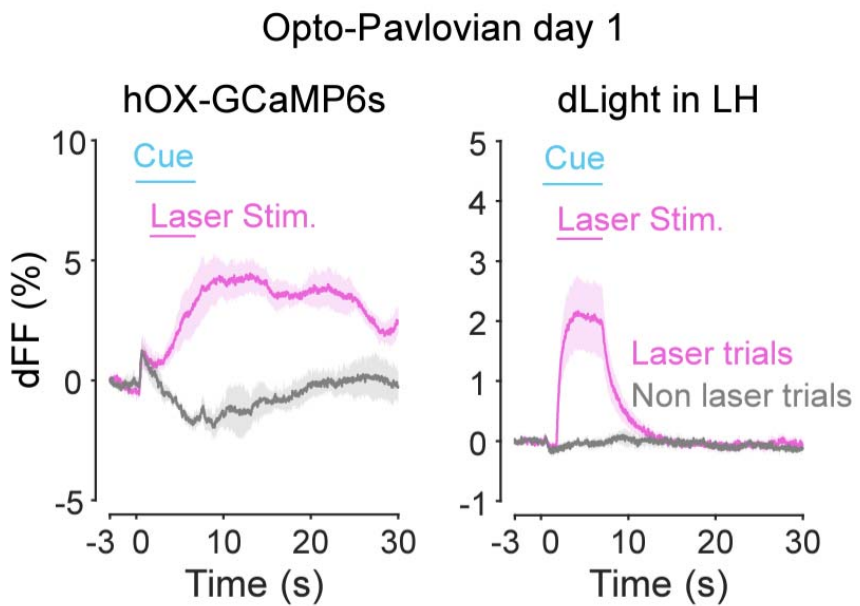


**Figure 5 - Figure Supplement 1.** Orexin-promoter GCaMP recording (left) and dLight recording during stimulation at session 1.

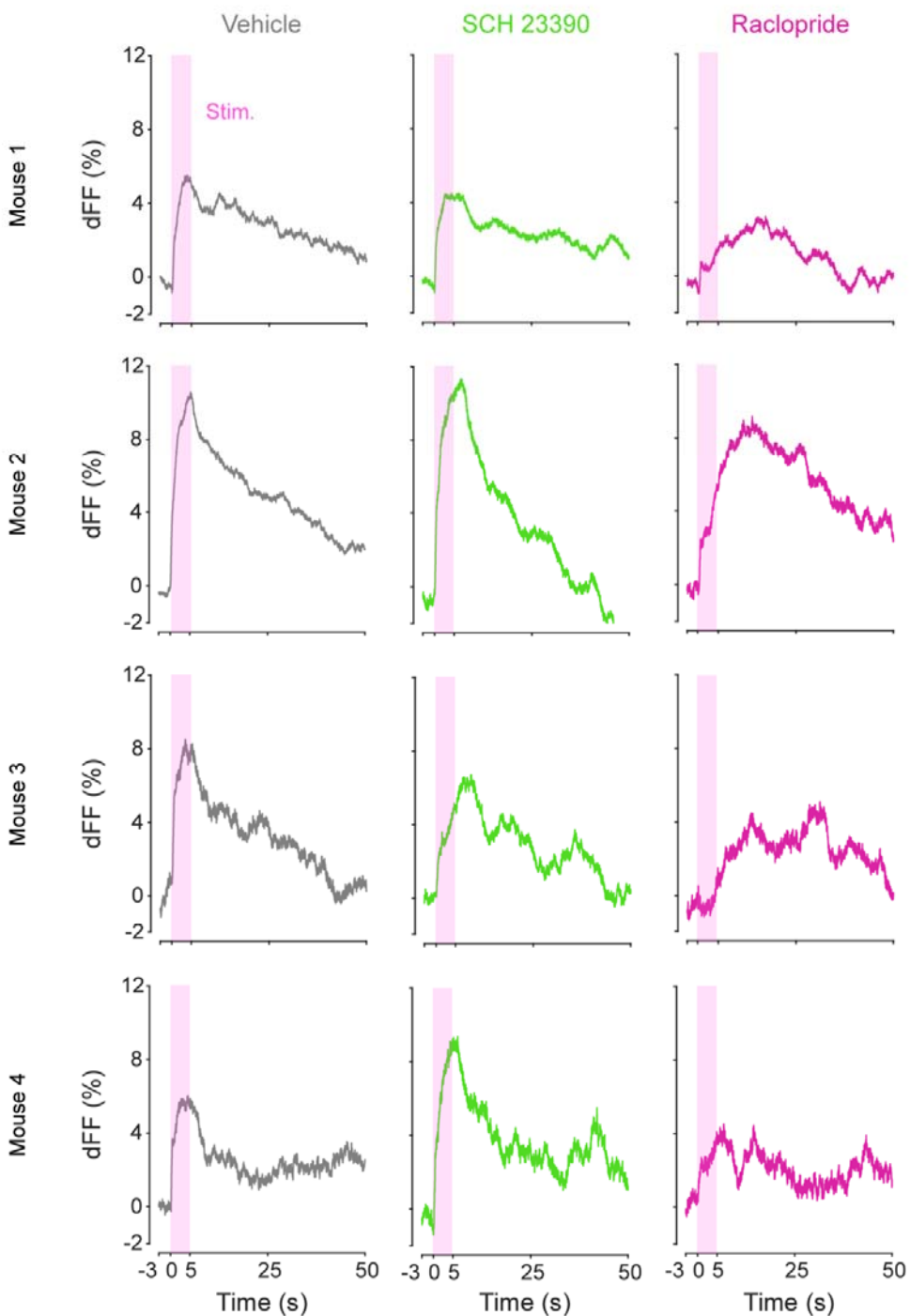


**Figure 6- Figure Supplement 1.** Individual traces for Figure 6E.

## References

1. Markowitz, J.E., Gillis, W.F., Jay, M., Wood, J., Harris, R.W., Cieszkowski, R., Scott, R., Brann, D., Koveal, D., Kula, T., et al. (2023). Spontaneous behaviour is structured by reinforcement without explicit reward. *Nature* *614*, 108–117. 10.1038/s41586-022-05611-2.
2. de Jong, J.W., Fraser, K.M., and Lammel, S. (2022). Mesoaccumbal Dopamine Heterogeneity: What Do Dopamine Firing and Release Have to Do with It? *Annu. Rev. Neurosci.* *45*, 109–129. 10.1146/annurev-neuro-110920-011929.
3. Yang, H., de Jong, J.W., Tak, Y., Peck, J., Bateup, H.S., and Lammel, S. (2018). Nucleus Accumbens Subnuclei Regulate Motivated Behavior via Direct Inhibition and Disinhibition of VTA Dopamine Subpopulations. *Neuron* *97*, 434-449.e4. 10.1016/j.neuron.2017.12.022.
4. Keiflin, R., and Janak, P.H. (2015). Dopamine Prediction Errors in Reward Learning and Addiction: From Theory to Neural Circuitry. *Neuron* *88*, 247–263. 10.1016/j.neuron.2015.08.037.
5. Tsai, H.-C., Zhang, F., Adamantidis, A., Stuber, G.D., Bonci, A., de Lecea, L., and Deisseroth, K. (2009). Phasic Firing in Dopaminergic Neurons Is Sufficient for Behavioral Conditioning. *Science* *324*, 1080–1084. 10.1126/science.1168878.
6. Lüscher, C., and Janak, P.H. (2021). Consolidating the Circuit Model for Addiction. *Annu. Rev. Neurosci.* *44*, 173–195. 10.1146/annurev-neuro-092920-123905.
7. Lüscher, C., Robbins, T.W., and Everitt, B.J. (2020). The transition to compulsion in addiction. *Nature Reviews Neuroscience* *21*, 247–263. 10.1038/s41583-020-0289-z.
8. Pascoli, V., Hiver, A., Li, Y., Harada, M., Esmaeili, V., and Lüscher, C. (2022). Cell-type specific synaptic plasticity in dorsal striatum is associated with punishment-resistance compulsive-like cocaine self-administration in mice. *Neuropsychopharmacology*. 10.1038/s41386-022-01429-8.
9. Nestler, E.J., and Carlezon, W.A. (2006). The Mesolimbic Dopamine Reward Circuit in Depression. *Biological Psychiatry* *59*, 1151–1159. 10.1016/j.biopsych.2005.09.018.
10. Krishnan, V., Han, M.-H., Graham, D.L., Berton, O., Renthal, W., Russo, S.J., LaPlant, Q., Graham, A., Lutter, M., Lagace, D.C., et al. (2007). Molecular Adaptations Underlying Susceptibility and Resistance to Social Defeat in Brain Reward Regions. *Cell* *131*, 391–404. 10.1016/j.cell.2007.09.018.
11. Deguchi, Y., Harada, M., Shinohara, R., Lazarus, M., Cherasse, Y., Urade, Y., Yamada, D., Sekiguchi, M., Watanabe, D., Furuyashiki, T., et al. (2016). mDia and ROCK Mediate Actin-Dependent Presynaptic Remodeling Regulating Synaptic Efficacy and Anxiety. *Cell Reports* *17*, 2405–2417. 10.1016/j.celrep.2016.10.088.
12. Kim, H.R., Malik, A.N., Mikhael, J.G., Bech, P., Tsutsui-Kimura, I., Sun, F., Zhang, Y., Li, Y., Watabe-Uchida, M., Gershman, S.J., et al. (2020). A Unified Framework for Dopamine Signals across Timescales. *Cell* *183*, 1600-1616.e25. 10.1016/j.cell.2020.11.013.

13. Patriarchi Tommaso, Cho Jounhong Ryan, Merten Katharina, Howe Mark W., Marley Aaron, Xiong Wei-Hong, Folk Robert W., Broussard Gerard Joey, Liang Ruqiang, Jang Min Jee, et al. (2018). Ultrafast neuronal imaging of dopamine dynamics with designed genetically encoded sensors. *Science* *360*, eaat4422. 10.1126/science.aat4422.
14. Howe, M.W., Tierney, P.L., Sandberg, S.G., Phillips, P.E.M., and Graybiel, A.M. (2013). Prolonged dopamine signalling in striatum signals proximity and value of distant rewards. *Nature* *500*, 575–579. 10.1038/nature12475.
15. Harada, M., Pascoli, V., Hiver, A., Flakowski, J., and Lüscher, C. (2021). Corticostriatal Activity Driving Compulsive Reward Seeking. *Biological Psychiatry* *90*, 808–818. 10.1016/j.biopsych.2021.08.018.
16. Pascoli, V., Hiver, A., Van Zessen, R., Loureiro, M., Achargui, R., Harada, M., Flakowski, J., and Lüscher, C. (2018). Stochastic synaptic plasticity underlying compulsion in a model of addiction. *Nature* *564*, 366–371. 10.1038/s41586-018-0789-4.
17. Saunders, B.T., Richard, J.M., Margolis, E.B., and Janak, P.H. (2018). Dopamine neurons create Pavlovian conditioned stimuli with circuit-defined motivational properties. *Nature Neuroscience* *21*, 1072–1083. 10.1038/s41593-018-0191-4.
18. Tan, K.R., Yvon, C., Turiault, M., Mirzabekov, J.J., Doehner, J., Labouëbe, G., Deisseroth, K., Tye, K.M., and Lüscher, C. (2012). GABA Neurons of the VTA Drive Conditioned Place Aversion. *Neuron* *73*, 1173–1183. 10.1016/j.neuron.2012.02.015.
19. van Zessen, R., Phillips, J.L., Budygin, E.A., and Stuber, G.D. (2012). Activation of VTA GABA Neurons Disrupts Reward Consumption. *Neuron* *73*, 1184–1194. 10.1016/j.neuron.2012.02.016.
20. Iino, Y., Sawada, T., Yamaguchi, K., Tajiri, M., Ishii, S., Kasai, H., and Yagishita, S. (2020). Dopamine D2 receptors in discrimination learning and spine enlargement. *Nature* *579*, 555–560. 10.1038/s41586-020-2115-1.
21. Lüscher, C., and Pascoli, V. (2021). ‘Ups, downs, and sideways’ of dopamine in drug addiction. *Trends in Neurosciences* *44*, 593–594. 10.1016/j.tins.2021.06.009.
22. Cohen, J.Y., Haesler, S., Vong, L., Lowell, B.B., and Uchida, N. (2012). Neuron-type-specific signals for reward and punishment in the ventral tegmental area. *Nature* *482*, 85–88. 10.1038/nature10754.
23. Schultz, W., Dayan, P., and Montague, P.R. (1997). A Neural Substrate of Prediction and Reward. *Science* *275*, 1593–1599. 10.1126/science.275.5306.1593.
24. Hasegawa, E., Miyasaka, A., Sakurai, K., Cherasse, Y., Li, Y., and Sakurai, T. (2022). Rapid eye movement sleep is initiated by basolateral amygdala dopamine signaling in mice. *Science* *375*, 994–1000. 10.1126/science.abl6618.
25. Vander Weele, C.M., Siciliano, C.A., Matthews, G.A., Namburi, P., Izadmehr, E.M., Espinel, I.C., Nieh, E.H., Schut, E.H.S., Padilla-Coreano, N., Burgos-Robles, A., et al. (2018). Dopamine enhances signal-to-noise ratio in cortical-brainstem encoding of aversive stimuli. *Nature* *563*, 397–401. 10.1038/s41586-018-0682-1.

26. Gyawali, U., Martin, D.A., Sun, F., Li, Y., and Calu, D. (2023). Dopamine in the dorsal bed nucleus of stria terminalis signals Pavlovian sign-tracking and reward violations. *eLife* 12, e81980. 10.7554/eLife.81980.
27. Chen, Y.-W., Morganstern, I., Barson, J.R., Hoebel, B.G., and Leibowitz, S.F. (2014). Differential Role of D1 and D2 Receptors in the Perifornical Lateral Hypothalamus in Controlling Ethanol Drinking and Food Intake: Possible Interaction with Local Orexin Neurons. *Alcoholism: Clinical and Experimental Research* 38, 777–786. 10.1111/acer.12313.
28. Gibson, G.D., Prasad, A.A., Jean-Richard-dit-Bressel, P., Yau, J.O.Y., Millan, E.Z., Liu, Y., Campbell, E.J., Lim, J., Marchant, N.J., Power, J.M., et al. (2018). Distinct Accumbens Shell Output Pathways Promote versus Prevent Relapse to Alcohol Seeking. *Neuron* 98, 512-520.e6. 10.1016/j.neuron.2018.03.033.
29. Harris, G.C., Wimmer, M., and Aston-Jones, G. (2005). A role for lateral hypothalamic orexin neurons in reward seeking. *Nature* 437, 556–559. 10.1038/nature04071.
30. Otis, J.M., Zhu, M., Namboodiri, V.M.K., Cook, C.A., Kosyk, O., Matan, A.M., Ying, R., Hashikawa, Y., Hashikawa, K., Trujillo-Pisanty, I., et al. (2019). Paraventricular Thalamus Projection Neurons Integrate Cortical and Hypothalamic Signals for Cue-Reward Processing. *Neuron* 103, 423-431.e4. 10.1016/j.neuron.2019.05.018.
31. Sharpe, M.J., Marchant, N.J., Whitaker, L.R., Richie, C.T., Zhang, Y.J., Campbell, E.J., Koivula, P.P., Necarsulmer, J.C., Mejias-Aponte, C., Morales, M., et al. (2017). Lateral Hypothalamic GABAergic Neurons Encode Reward Predictions that Are Relayed to the Ventral Tegmental Area to Regulate Learning. *Current Biology* 27, 2089-2100.e5. 10.1016/j.cub.2017.06.024.
32. James, M.H., Stopper, C.M., Zimmer, B.A., Koll, N.E., Bowrey, H.E., and Aston-Jones, G. (2019). Increased Number and Activity of a Lateral Subpopulation of Hypothalamic Orexin/Hypocretin Neurons Underlies the Expression of an Addicted State in Rats. *Biological Psychiatry* 85, 925–935. 10.1016/j.biopsych.2018.07.022.
33. O'Connor, E.C., Kremer, Y., Lefort, S., Harada, M., Pascoli, V., Rohner, C., and Lüscher, C. (2015). Accumbal D1R Neurons Projecting to Lateral Hypothalamus Authorize Feeding. *Neuron* 88, 553–564. 10.1016/j.neuron.2015.09.038.
34. Jennings, J.H., Ung, R.L., Resendez, S.L., Stamatakis, A.M., Taylor, J.G., Huang, J., Veleta, K., Kantak, P.A., Aita, M., Shilling-Scrivo, K., et al. (2015). Visualizing Hypothalamic Network Dynamics for Appetitive and Consummatory Behaviors. *Cell* 160, 516–527. 10.1016/j.cell.2014.12.026.
35. Jennings, J.H., Rizzi, G., Stamatakis, A.M., Ung, R.L., and Stuber, G.D. (2013). The Inhibitory Circuit Architecture of the Lateral Hypothalamus Orchestrates Feeding. *Science* 341, 1517–1521. 10.1126/science.1241812.
36. Marino, R.A.M., McDevitt, R.A., Gantz, S.C., Shen, H., Pignatelli, M., Xin, W., Wise, R.A., and Bonci, A. (2020). Control of food approach and eating by a GABAergic

projection from lateral hypothalamus to dorsal pons. *Proceedings of the National Academy of Sciences* *117*, 8611–8615. 10.1073/pnas.1909340117.

37. Yang, Y.-L., Ran, X.-R., Li, Y., Zhou, L., Zheng, L.-F., Han, Y., Cai, Q.-Q., Wang, Z.-Y., and Zhu, J.-X. (2019). Expression of Dopamine Receptors in the Lateral Hypothalamic Nucleus and Their Potential Regulation of Gastric Motility in Rats With Lesions of Bilateral Substantia Nigra. *Frontiers in Neuroscience* *13*.

38. Mickelsen, L.E., Bolisetty, M., Chimileski, B.R., Fujita, A., Beltrami, E.J., Costanzo, J.T., Naparstek, J.R., Robson, P., and Jackson, A.C. (2019). Single-cell transcriptomic analysis of the lateral hypothalamic area reveals molecularly distinct populations of inhibitory and excitatory neurons. *Nature Neuroscience* *22*, 642–656. 10.1038/s41593-019-0349-8.

39. González, J.A., Iordanidou, P., Strom, M., Adamantidis, A., and Burdakov, D. (2016). Awake dynamics and brain-wide direct inputs of hypothalamic MCH and orexin networks. *Nature Communications* *7*, 11395. 10.1038/ncomms11395.

40. Borgland, S.L., Taha, S.A., Sarti, F., Fields, H.L., and Bonci, A. (2006). Orexin A in the VTA Is Critical for the Induction of Synaptic Plasticity and Behavioral Sensitization to Cocaine. *Neuron* *49*, 589–601. 10.1016/j.neuron.2006.01.016.

41. Bubser, M., Fadel, J.R., Jackson, L.L., Meador-Woodruff, J.H., Jing, D., and Deutch, A.Y. (2005). Dopaminergic regulation of orexin neurons. *European Journal of Neuroscience* *21*, 2993–3001. 10.1111/j.1460-9568.2005.04121.x.

42. Thomas, C.S., Mohammadkhani, A., Rana, M., Qiao, M., Baimel, C., and Borgland, S.L. (2022). Optogenetic stimulation of lateral hypothalamic orexin/dynorphin inputs in the ventral tegmental area potentiates mesolimbic dopamine neurotransmission and promotes reward-seeking behaviours. *Neuropsychopharmacology* *47*, 728–740. 10.1038/s41386-021-01196-y.

43. Baimel, C., Lau, B.K., Qiao, M., and Borgland, S.L. (2017). Projection-Target-Defined Effects of Orexin and Dynorphin on VTA Dopamine Neurons. *Cell Reports* *18*, 1346–1355. 10.1016/j.celrep.2017.01.030.

44. Yamanaka, A., Muraki, Y., Ichiki, K., Tsujino, N., Kilduff, T.S., Goto, K., and Sakurai, T. (2006). Orexin Neurons Are Directly and Indirectly Regulated by Catecholamines in a Complex Manner. *Journal of Neurophysiology* *96*, 284–298. 10.1152/jn.01361.2005.

45. Ying Li and Anthony N. van den Pol (2005). Direct and Indirect Inhibition by Catecholamines of Hypocretin/Orexin Neurons. *J. Neurosci.* *25*, 173. 10.1523/JNEUROSCI.4015-04.2005.

46. Linehan, V., Trask, R.B., Briggs, C., Rowe, T.M., and Hirasawa, M. (2015). Concentration-dependent activation of dopamine receptors differentially modulates GABA release onto orexin neurons. *European Journal of Neuroscience* *42*, 1976–1983. 10.1111/ejn.12967.

47. Linehan, V., Rowe, T.M., and Hirasawa, M. (2019). Dopamine modulates excitatory transmission to orexin neurons in a receptor subtype-specific manner. *American Journal of*

Physiology-Regulatory, Integrative and Comparative Physiology 316, R68–R75. 10.1152/ajpregu.00150.2018.

48. Feng, J., Zhang, C., Lischinsky, J.E., Jing, M., Zhou, J., Wang, H., Zhang, Y., Dong, A., Wu, Z., Wu, H., et al. (2019). A Genetically Encoded Fluorescent Sensor for Rapid and Specific In Vivo Detection of Norepinephrine. *Neuron* 102, 745–761.e8. 10.1016/j.neuron.2019.02.037.

49. Sun, F., Zhou, J., Dai, B., Qian, T., Zeng, J., Li, X., Zhuo, Y., Zhang, Y., Wang, Y., Qian, C., et al. (2020). Next-generation GRAB sensors for monitoring dopaminergic activity in vivo. *Nature Methods* 17, 1156–1166. 10.1038/s41592-020-00981-9.

50. Zhuo, Y., Luo, B., Yi, X., Dong, H., Miao, X., Wan, J., Williams, J.T., Campbell, M.G., Cai, R., Qian, T., et al. (2023). Improved green and red GRAB sensors for monitoring dopaminergic activity in vivo. *Nature Methods*. 10.1038/s41592-023-02100-w.

51. Wu, Z., Lin, D., and Li, Y. (2022). Pushing the frontiers: tools for monitoring neurotransmitters and neuromodulators. *Nature Reviews Neuroscience* 23, 257–274. 10.1038/s41583-022-00577-6.

52. Patriarchi, T., Mohebi, A., Sun, J., Marley, A., Liang, R., Dong, C., Puhger, K., Mizuno, G.O., Davis, C.M., Wiltgen, B., et al. (2020). An expanded palette of dopamine sensors for multiplex imaging in vivo. *Nature Methods* 17, 1147–1155. 10.1038/s41592-020-0936-3.

53. Mohebi, A., Pettibone, J.R., Hamid, A.A., Wong, J.-M.T., Vinson, L.T., Patriarchi, T., Tian, L., Kennedy, R.T., and Berke, J.D. (2019). Dissociable dopamine dynamics for learning and motivation. *Nature* 570, 65–70. 10.1038/s41586-019-1235-y.

54. Liu, C., Cai, X., Ritzau-Jost, A., Kramer, P.F., Li, Y., Khaliq, Z.M., Hallermann, S., and Kaeser, P.S. (2022). An action potential initiation mechanism in distal axons for the control of dopamine release. *Science* 375, 1378–1385. 10.1126/science.abn0532.

55. Nieh, E.H., Matthews, G.A., Allsop, S.A., Presbrey, K.N., Leppla, C.A., Wichmann, R., Neve, R., Wildes, C.P., and Tye, K.M. (2015). Decoding Neural Circuits that Control Compulsive Sucrose Seeking. *Cell* 160, 528–541. 10.1016/j.cell.2015.01.003.

56. Ed F. Bracey, Nikola Grujic, Daria Peleg-Raibstein, and Denis Burdakov (2022). Coding of reward uncertainty and probability by orexin neurons. *bioRxiv*, 2022.04.13.488195. 10.1101/2022.04.13.488195.

57. Viskaitis, P., Arnold, M., Garau, C., Jensen, L.T., Fugger, L., Peleg-Raibstein, D., and Burdakov, D. (2022). Ingested non-essential amino acids recruit brain orexin cells to suppress eating in mice. *Current Biology* 32, 1812–1821.e4. 10.1016/j.cub.2022.02.067.

58. Li, H.-T., Donegan, D.C., Peleg-Raibstein, D., and Burdakov, D. (2022). Hypothalamic deep brain stimulation as a strategy to manage anxiety disorders. *Proceedings of the National Academy of Sciences* 119, e2113518119. 10.1073/pnas.2113518119.

59. González, J.A., Jensen, L.T., Iordanidou, P., Strom, M., Fugger, L., and Burdakov, D. (2016). Inhibitory Interplay between Orexin Neurons and Eating. *Current Biology* *26*, 2486–2491. 10.1016/j.cub.2016.07.013.
60. Karnani, M.M., Schöne, C., Bracey, E.F., González, J.A., Viskaitis, P., Li, H.-T., Adamantidis, A., and Burdakov, D. (2020). Role of spontaneous and sensory orexin network dynamics in rapid locomotion initiation. *Progress in Neurobiology* *187*, 101771. 10.1016/j.pneurobio.2020.101771.
61. Donegan, D., Peleg-Raibstein, D., Lambercy, O., and Burdakov, D. (2022). Anticipatory counteracting of motor challenges by premovement activation of orexin neurons. *PNAS Nexus* *1*, pgac240. 10.1093/pnasnexus/pgac240.
62. Yonemochi, N., Ardianto, C., Yang, L., Yamamoto, S., Ueda, D., Kamei, J., Waddington, J.L., and Ikeda, H. (2019). Dopaminergic mechanisms in the lateral hypothalamus regulate feeding behavior in association with neuropeptides. *Biochemical and Biophysical Research Communications* *519*, 547–552. 10.1016/j.bbrc.2019.09.037.
63. Verharen, J.P.H., Zhu, Y., and Lammel, S. (2020). Aversion hot spots in the dopamine system. *Current Opinion in Neurobiology* *64*, 46–52. 10.1016/j.conb.2020.02.002.
64. Lutas, A., Kucukdereli, H., Alturkistani, O., Carty, C., Sugden, A.U., Fernando, K., Diaz, V., Flores-Maldonado, V., and Andermann, M.L. (2019). State-specific gating of salient cues by midbrain dopaminergic input to basal amygdala. *Nature Neuroscience* *22*, 1820–1833. 10.1038/s41593-019-0506-0.
65. Yamashita, A., Moriya, S., Nishi, R., Kaminosono, J., Yamanaka, A., and Kuwaki, T. (2021). Aversive emotion rapidly activates orexin neurons and increases heart rate in freely moving mice. *Molecular Brain* *14*, 104. 10.1186/s13041-021-00818-2.
66. Ford, C.P. (2014). The role of D2-autoreceptors in regulating dopamine neuron activity and transmission. *Neuroscience* *282*, 13–22. 10.1016/j.neuroscience.2014.01.025.
67. Loris L. Ferrari, Daniel Park, Lin Zhu, Matthew R. Palmer, Rebecca Y. Broadhurst, and Elda Arrigoni (2018). Regulation of Lateral Hypothalamic Orexin Activity by Local GABAergic Neurons. *J. Neurosci.* *38*, 1588. 10.1523/JNEUROSCI.1925-17.2017.
68. Burt, J., Alberto, C.O., Parsons, M.P., and Hirasawa, M. (2011). Local network regulation of orexin neurons in the lateral hypothalamus. *American Journal of Physiology-Regulatory, Integrative and Comparative Physiology* *301*, R572–R580. 10.1152/ajpregu.00674.2010.
69. Thoeni, S., Loureiro, M., O'Connor, E.C., and Lüscher, C. (2020). Depression of Accumbal to Lateral Hypothalamic Synapses Gates Overeating. *Neuron* *107*, 158-172.e4. 10.1016/j.neuron.2020.03.029.
70. Womer, D.E., Jones, B.C., and Gene Erwin, V. (1994). Characterization of dopamine transporter and locomotor effects of cocaine, GBR 12909, epidepride, and SCH 23390 in C57BL and DBA mice. *Pharmacology Biochemistry and Behavior* *48*, 327–335. 10.1016/0091-3057(94)90534-7.

71. Simón, V.M., Parra, A., Miñarro, J., Arenas, M.C., Vinader-Caerols, C., and Aguilar, M.A. (2000). Predicting how equipotent doses of chlorpromazine, haloperidol, sulpiride, raclopride and clozapine reduce locomotor activity in mice. *European Neuropsychopharmacology* *10*, 159–164. 10.1016/S0924-977X(00)00070-5.
72. Mingote, S., Chuhma, N., Kalmbach, A., Thomsen, G.M., Wang, Y., Mihali, A., Sferrazza, C., Zucker-Scharff, I., Siena, A.-C., Welch, M.G., et al. (2017). Dopamine neuron dependent behaviors mediated by glutamate cotransmission. *eLife* *6*, e27566. 10.7554/eLife.27566.
73. Zell, V., Steinkellner, T., Hollon, N.G., Warlow, S.M., Souter, E., Faget, L., Hunker, A.C., Jin, X., Zweifel, L.S., and Hnasko, T.S. (2020). VTA Glutamate Neuron Activity Drives Positive Reinforcement Absent Dopamine Co-release. *Neuron* *107*, 864-873.e4. 10.1016/j.neuron.2020.06.011.
74. Dal Bo, G., St-Gelais, F., Danik, M., Williams, S., Cotton, M., and Trudeau, L.-E. (2004). Dopamine neurons in culture express VGLUT2 explaining their capacity to release glutamate at synapses in addition to dopamine. *Journal of Neurochemistry* *88*, 1398–1405. 10.1046/j.1471-4159.2003.02277.x.
75. Melani, R., and Tritsch, N.X. (2022). Inhibitory co-transmission from midbrain dopamine neurons relies on presynaptic GABA uptake. *Cell Reports* *39*, 110716. 10.1016/j.celrep.2022.110716.
76. Zhang, Y., Rózsa, M., Liang, Y., Bushey, D., Wei, Z., Zheng, J., Reep, D., Broussard, G.J., Tsang, A., Tsegaye, G., et al. (2023). Fast and sensitive GCaMP calcium indicators for imaging neural populations. *Nature* *615*, 884–891. 10.1038/s41586-023-05828-9.
77. Baik, J.-H. (2013). Dopamine Signaling in reward-related behaviors. *Frontiers in Neural Circuits* *7*.
78. Garau, C., Blomeley, C., and Burdakov, D. (2020). Orexin neurons and inhibitory AgRP→orexin circuits guide spatial exploration in mice. *The Journal of Physiology* *598*, 4371–4383. 10.1113/JP280158.
79. Ivy B. Hoang, Joseph J. Munier, Anna Verghese, Zara Greer, Samuel J. Millard, Lauren E. DiFazio, Courtney Sercander, Alicia Izquierdo, and Melissa J. Sharpe (2023). A novel hypothalamic-midbrain circuit for model-based learning. *bioRxiv*, 2023.03.02.530856. 10.1101/2023.03.02.530856.
80. Sakurai, T. (2014). The role of orexin in motivated behaviours. *Nature Reviews Neuroscience* *15*, 719–731. 10.1038/nrn3837.
81. Keefer, S.E., Cole, S., and Petrovich, G.D. (2016). Orexin/hypocretin receptor 1 signaling mediates Pavlovian cue-food conditioning and extinction. *Physiology & Behavior* *162*, 27–36. 10.1016/j.physbeh.2016.02.042.
82. Sharf, R., Sarhan, M., Brayton, C.E., Guarnieri, D.J., Taylor, J.R., and DiLeone, R.J. (2010). Orexin Signaling Via the Orexin 1 Receptor Mediates Operant Responding for Food Reinforcement. *Biological Psychiatry* *67*, 753–760. 10.1016/j.biopsych.2009.12.035.

